SCIENCE CHINA
Information Sciences

• RESEARCH PAPER •

May 2024, Vol. 67, Iss. 5, 152302:1–152302:16
https://doi.org/10.1007/s11432-023-3950-0

Carbon efficiency modeling and optimization of solar-powered cellular networks

Yuxi ZHAO[1], Xiaohu GE[1], Wen YAN[2], Tao HAN[1*] & Yi ZHONG[1*]

[1]*School of Electronic Information and Communications, Huazhong University of Science and Technology, Wuhan* 430074*, China;*
[2]*Huawei Technology Co., Ltd., Shanghai* 201206*, China.*

Received 4 July 2023/Revised 21 November 2023/Accepted 30 January 2024/Published online 23 April 2024

Abstract As wireless communication traffic experiences rapid growth, the carbon emissions caused by the communication industry are also on the rise. To achieve "carbon neutrality", researchers are considering the use of renewable energy sources to power cellular networks, thereby reducing carbon emissions. However, a challenge arises when using renewable energy, specifically owing to the unpredictable nature of both the energy consumption of the cellular network and the power generation from renewable sources. This inconsistency results in low renewable energy utilization and reduced carbon efficiency. Herein, we construct a carbon efficiency model of solar-powered cellular networks using practical data from solar radiation. We propose a mechanism that alternately optimizes the performance of the renewable energy network and the cellular network. This approach is based on convex optimization theory and the Dinkelback algorithm, and it leads to the design of a carbon efficiency optimization algorithm. This algorithm aims to improve the carbon efficiency of cellular networks and reduce their carbon emissions. Simulation results demonstrate that our optimization scheme yields a maximum improvement of 2.56×10^8 bps/g in the carbon efficiency of the cellular network as compared to conventional power allocation schemes such as the traditional water filling method and heuristic energy sharing and charge/discharge algorithms.

Keywords cellular networks, renewable energy, carbon efficiency, convex optimization theory, dinkelbach

1 Introduction

The Paris Agreement, ratified by 197 nations on December 12, 2015, during the Conference of the Parties in Paris, stands as a strong commitment to global endeavors toward green, low-carbon, climate-resilient, and sustainable development. International organizations like the International Telecommunication Union and the Global System for Mobile Communications Association are championing this case, urging the global information and communications technology industry to reduce carbon emissions by 45% by 2030 [1]. A significant proportion of carbon emissions from cellular networks comes from scope 2 emissions, which are produced during the manufacturing process of the outsourced electricity used [2]. Notably, a study presented in the Huawei 5G white paper reveals that a 5G base station (BS) consumes around 300% to 350% more power than a 4G BS [3]. As the 5G network expands, this will inevitably lead to an increase in cellular network carbon emissions. To counteract this, the integration of distributed renewable energy sources, such as solar energy, into BSs for the energy consumption of cellular networks is proposed [4,5]. However, on the supply side, the power generation system of distributed renewable energy forms a renewable energy network. This network has inherent drawbacks such as volatility, intermittency, and unpredictability [6]. On the demand side, the BSs form a cellular network, with energy dictated by random traffic [7]. This variability makes it difficult to match the power generation of renewable energy with the energy consumption of BSs, resulting in a low utilization rate of renewable energy. It presents a significant challenge to simultaneously optimize the performance of both the renewable energy network and the cellular network to improve the carbon efficiency (CE) of cellular networks powered by renewable energy.

* Corresponding author (email: hantao@hust.edu.cn, yzhong@hust.edu.cn)

To meet the above challenge, it is necessary to find a feasible solution to match the energy supply of renewable sources with the energy demand of BSs. In other words, we need to align the energy flow of renewable energy networks with the information flow of cellular networks. From the perspective of the renewable energy network, optimized architectures of renewable energy have been proposed for powering wireless networks [8–11]. For instance, an energy cooperation model combining traditional grid power and renewable energy was proposed for cellular networks, considering limited energy storage [8]. In remote areas of Bangladesh, where wind and photovoltaic characteristics are distinctive, an energy cooperation framework was proposed for hybrid photovoltaic wind-supplied long-term evolution BSs [9]. The sustainability, cost-effectiveness, and energy efficiency of diesel generators and photovoltaic supply for off-grid BSs were discussed in [10]. Based on average and complete network reachable statistics, an inter-BS physical power line deployment algorithm was proposed [11]. An energy-sharing algorithm for wireless networks powered by renewable energy has also been investigated in [12, 13]. One such study utilized interior point methods to reduce energy costs, proposing an energy cooperation scheme based on wind and photovoltaic energy supply models [12]. Another study suggested an energy-sharing strategy to improve energy efficiency and supply stability while reducing carbon emissions in off-grid cellular networks [13].

From the perspective of the cellular network, various control algorithms for BSs have been proposed to optimize the performance of renewable energy-powered wireless networks [6, 14–16]. For instance, one proposal [14] suggested using harvested energy to minimize grid power consumption through BS deployment and power control. Another study [15] proposed a wireless network resource allocation approach based on the Dinkelbach method, optimizing both time and power resources. To minimize the weighted sum of the grid energy cost and the packet drop cost, a greedy assignment algorithm and a heuristic online policy were proposed [16]. In addition, an adaptive resource management and user access control algorithm was put forward to solve the randomness of renewable energy and enhance the sustainability of wireless networks [6].

However, these studies primarily focused on either renewable energy networks or cellular networks without considering the joint optimization of both. To address this gap, a study [17] investigated a user access algorithm designed to minimize the total energy consumption of cellular networks. Another study [18] designed a BS states control algorithm, which optimized system energy consumption by sharing energy within a microgrid composed of BSs. Certain studies have shown a particular interest in reducing grid power consumption, as this area produces a greater amount of carbon emissions than power generated by renewable sources. By jointly optimizing the transmission power and user access mechanisms in cellular networks, energy sharing and traffic shifting approaches were proposed to minimize grid energy consumption for cellular networks [19]. Lagrangian dual decomposition and meta-heuristic algorithms were used to solve BS power allocation and energy cooperative the optimization problems [20]. A framework for energy cooperation among BSs in coordinated multipoint (CoMP) transmission-based cellular networks was proposed [21], allowing renewable energy to be shared among BSs. This network integrates a dynamic point selection CoMP technique for selecting the best-serving BSs for user equipment. However, these studies have not considered the energy storage configuration nor the charging and discharging of batteries for optimizing CE in cellular networks powered by renewable energy.

To improve CE, we propose joint CE optimization algorithms for solar-powered cellular networks. The main contributions of this paper are summarized as follows:

- Drawing on practical data, a power generation model of solar energy has been proposed for renewable energy networks. Furthermore, a CE model specifically designed for solar-powered cellular networks has been proposed. Here, CE is defined as the ratio of the total downlink throughput of cellular networks to their carbon emissions.
- An alternative CE optimization scheme has been developed for these solar-powered cellular networks. Using the interior point approach, this scheme includes an energy-sharing algorithm and a charge/discharge algorithm among BSs to reduce traditional grid power consumption and improve carbon emissions in solar-powered cellular networks. To further improve CE, a BS transmission power allocation algorithm has been proposed, which is based on the Lagrangian dual and Dinkelbach methods.
- The simulation results show that after implementing our optimization scheme, the CE of the cellular network showed a maximum improvement of 2.56×10^8 bps/g compared with the cellular network using the traditional water filling power allocation scheme and heuristic energy sharing and charge/discharge algorithms.

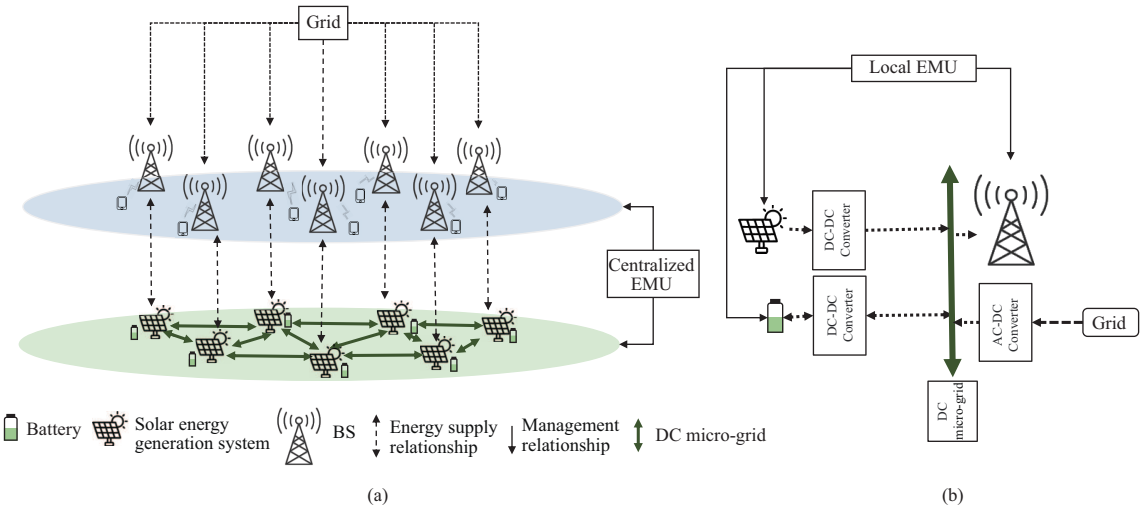

Figure 1 (Color online) (a) Solar-powered cellular networks; (b) solar-powered BS architecture.

2 System model

We have a similar scenario with [5,8,22] which is shown in Figure 1. Figure 1(a) shows the solar-powered cellular network that consisting of N BSs integrated with distributed power generation systems of solar energy which can supply renewable energy to the BSs. BSs can be powered by both renewable source and traditional grid power. Besides, each BS is integrated with an energy storage system with limited capacity. Because the solar energy is only abundant during the daytime, the energy storage system can store the energy generated by the solar power during the daytime and discharge it at night. As solar power systems generate direct current (DC) and BSs are powered by DC, connecting BSs via DC power lines to form a DC micro-grid is a logical approach. Despite DC being less stable than AC, DC micro-grids have been successfully deployed in many areas over short distances [23]. Within the network, a centralized energy management unit (EMU) assumes the responsibility of collectively managing the energy supply from the renewable energy network and the energy consumption of the cellular network. The EMU is equipped to make informed decisions concerning energy sharing and the power control scheme for BS energy consumption. Figure 1(b) illustrates the solar-powered BSs architecture. The grid power is connected to the DC micro-grid through the alternating current-direct current (AC-DC) converter. Given that the output voltage of the solar power generation system and the energy storage battery differs from that required by the BSs, a DC-DC converter is employed to adjust the voltage before powering the BSs. Each BS is integrated with a local EMU, which can receive instructions from the centralized EMU and manage the BS, solar power generation system, and energy storage system.

2.1 Solar energy generation model

We consider a discrete time system where the time is divided into multiple time slots with slot index t, and the length of a time slot is the unit time Δt. The average power generated by the power generation system of solar energy integrated by BS_i at time slot t is [24,25]

$$P_{\mathrm{RE}(i)}(t) = H_i(t)\lambda A, \tag{1}$$

where $P_{\mathrm{RE}(i)}$ is the average power at the time slot t generated by the generation system of solar energy integrated at BS_i, A is the area of solar photovoltaic panels, λ is the efficiency of the solar photovoltaic panel, $H_i(t)$ is the solar radiation on the panels at the time slot t and BS_i. It can be seen from (1) that the generated power has a linear relationship with the solar radiation intensity.

Based on the solar radiation data provided by the European Centre for Medium-Range Weather Forecasts [26], the hourly variations of solar radiation at Jianghan District, Wuhan City in spring, summer, autumn, and winter are plotted in Figure 2.

It can be seen from Figure 2 that the hourly variation of the solar radiation is periodic. Besides, the solar radiation in summer is larger than that in spring, autumn, and winter. However, because of the

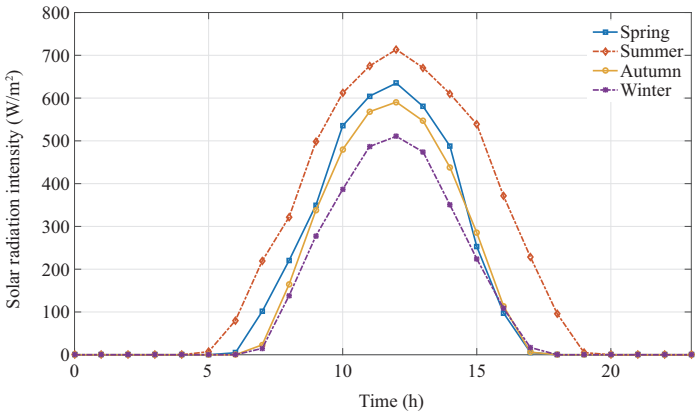

Figure 2 (Color online) Solar radiation time series changed hour-by-hour.

Table 1 Solar radiation model parameters

Season	a	b	c
Spring	3979.25	2.40	11.72
Summer	5820.65	3.38	12.09
Autumn	3671.52	2.35	11.84
Winter	3069.08	2.31	11.86

influence of clouds cover, the hourly variation of the solar radiation fluctuates based on periodic variations which can affect the solar radiation in different space distributions.

The Gaussian distribution is usually used to fit the daily variation of solar radiation, and it has been proven to be suitable for most regions in [27, 28]. The cloud shading factor is used to simulate the occlusion of clouds [29]. The solar radiation model is as follows:

$$H_i(t) = S_i(t)a\frac{1}{\sqrt{2\pi}b}\mathrm{e}^{-\left(\frac{(t-c)^2}{2b^2}\right)}, \tag{2}$$

where a, b are parameters of Gaussian distribution, $S_i(t)$ represents the cloud shading factor of BS_i at the time slot t. The parameters of Gaussian distribution in this paper are given in Table 1, which are obtained by MATLAB using the data in Figure 2. $S_i(t)$ is calculated as

$$S_i(t) = a_1 r_i(t)^2 + a_2 r_i(t) + a_3, \tag{3}$$

where a_1, a_2, a_3 are parameters that depend on the region and the season, $r_i(t)$ is the cloud cover over BS_i at the time slot t.

2.2 Energy storage model

The battery is considered as the energy storage system in this paper. The main characterization parameter of the battery energy storage system is the energy state $B_i(t)$ which represents the battery energy of BS_i at the time slot t. There are the upper charge threshold E_{Bmax} and the lower discharge threshold E_{Bmin} which represent the maximum energy storage and the minimum energy storage of the battery respectively. When the upper charge threshold is exceeded, the battery will enter into the overcharge state. On the contrary, when the energy of the battery is lower than the lower discharge threshold, the battery will enter into the over-discharge state. The lower discharge threshold is determined by the depth of discharge (DOD) $E_{\mathrm{Bmin}} = (1-\mathrm{DOD}) \times E_{\mathrm{Bmax}}$. There are two efficiencies in the charging and discharging processes of the battery, i.e., the charging efficiency and the discharging efficiency. The charging efficiency refers to the ratio between the actual charging power received by the battery and the charging power supplied by the energy source during the charging process. The discharging efficiency refers to the ratio between the discharge power received by the load and the discharge power supplied by the battery during the discharging process. Therefore, the actual charging power received by the battery is computed as the product of the charging power supplied by the energy source and the charging efficiency. Conversely, the actual discharging power received by the load is determined by the product of the discharging power

supplied by the battery and the discharging efficiency. The discharging power supplied by the battery remains unaffected by the discharging efficiency. It is assumed that the charging efficiency of the battery is equal to the discharging efficiency denoted as μ.

The energy of the battery in BS_i at the end of the time slot t is calculated in

$$B_i(t) = B_i(t-\Delta t) + \Delta t \times \mu \times C_i(t) - \Delta t \times D_i(t), \tag{4a}$$

$$\text{s.t.} \quad E_{\mathrm{Bmin}} \leqslant B_i(t) \leqslant E_{\mathrm{Bmax}}, \tag{4b}$$

$$C_i(t) \geqslant 0,\ D_i(t) \geqslant 0, \tag{4c}$$

$$C_i(t) \times D_i(t) = 0, \tag{4d}$$

where $C_i(t)$ represents the average charging power supplied by the energy source in BS_i at the time slot t, $D_i(t)$ represents the average discharging power of the battery in at the time slot t.

2.3 BS energy consumption model

It is assumed that each BS has M antennas. The users and BSs follow the Poisson point processes (PPP) with density λ_u and λ_b respectively. The users access the nearest BS, so the coverage area of a BS is a Voronoi polygon [30–32]. The channel matrix of BS_i is $\boldsymbol{G}_i \in \mathbb{C}^{K_i(t)\times M}$, where $\mathbb{C}$ represents the set of complex numbers, K_i is the number of users within coverage area of BS_i. $\mathbb{C}^{K_i(t)\times M}$ represents the $K_i(t) \times M$ dimensional matrix in the complex number domain

$$\boldsymbol{G}_i = \boldsymbol{F}_i^{\frac{1}{2}} \boldsymbol{H}_i, \tag{5a}$$

$$\boldsymbol{H}_i = \begin{bmatrix} \boldsymbol{h}_{(i,1)} \\ \vdots \\ \boldsymbol{h}_{(i,K_i(t))} \end{bmatrix}, \tag{5b}$$

where $\boldsymbol{F}_i = \mathrm{diag}\left[\beta_{(i,1)}, \beta_{(i,2)}, \ldots, \beta_{(i,K_i(t))}\right]$, $\beta_{(i,k)}$ represents the large-scale fading channel matrix between the kth user and the BS_i, $\beta_{(i,k)} = \frac{\phi\zeta}{d_{(i,k)}^{\alpha}}$, $d_{(i,k)}$ represents the distance between the kth user and the BS_i, α is the path loss coefficient, ϕ is constant related to the carrier frequency and the antenna gain, ζ is a log-normal shadow fading variable, $10\log_{10}\zeta \sim \mathcal{N}\left(0, \sigma_{\mathrm{sh}}^2\right)$. $\boldsymbol{H}_i \in \mathbb{C}^{K_i(t)\times M}$ is Rayleigh fading matrix, $\boldsymbol{H}_i \sim \exp(1)$, $\boldsymbol{h}_{(i,k)} \in \mathbb{C}^{1\times M}$.

We assume that the BSs use the zero-forcing (ZF) precoding which can effectively eliminate intra cell interference. The signal received by users access the BS_i at the time slot t is

$$\boldsymbol{y}_i = \boldsymbol{G}_i \boldsymbol{W}_i \boldsymbol{P}_{\mathrm{t}(i)}^{\frac{1}{2}} \boldsymbol{x}_i + \boldsymbol{n}_i, \tag{6}$$

where $\boldsymbol{x}_i$ is the transmission signal vector of BS_i, $\boldsymbol{W}_i$ is ZF precoding matrix, $\overline{\boldsymbol{W}}_i = \boldsymbol{H}_i^{\mathrm{H}}(\boldsymbol{H}_i\boldsymbol{H}_i^{\mathrm{H}})^{-1}$, $\boldsymbol{W}_i = [\boldsymbol{w}_{1(i)}, \boldsymbol{w}_{2(i)}, \ldots, \boldsymbol{w}_{K(i)}], \boldsymbol{w}_{k(i)} = \frac{\overline{\boldsymbol{w}}_k(i)}{\|\overline{\boldsymbol{w}}_k(i)\|}$, $\overline{\boldsymbol{w}}_k(i)$ is the kth column vector of $\overline{\boldsymbol{W}}_i$, $\boldsymbol{P}_{\mathrm{t}(i)}$ is the transmission power vector of BS_i. $\boldsymbol{n}_i$ is the additive white Gaussian noise.

In inter cell, the adaptive partial frequency multiplexing technology is used to avoid the same frequency band used by adjacent cells, so the inter cell interference can be eliminated effectively [33]. So the signal-to-noise ratio (SNR) received by kth user from BS_i is

$$\theta_{i,k} = \frac{\beta_{(i,k)} P_{\mathrm{t}(i,k)}(t)}{\sigma^2 \left\|\overline{\boldsymbol{w}}_k(i)\right\|^2}. \tag{7}$$

Because the users access the nearest BS, so the probability density function of the distance between the kth user and the BS_i is

$$f_{d_{i,k}}(r) = \mathrm{e}^{-\lambda_b \pi r^2} 2\pi\lambda_b r. \tag{8}$$

Based on this, we can get

$$\boldsymbol{E}\left[\beta_{(i,k)}\right] = \boldsymbol{E}\left[d_{(i,k)}^{-\alpha}\right] \phi \boldsymbol{E}\left[\zeta\right]$$

$$= \frac{\pi^{\frac{\alpha}{2}} \left(-\lambda_b\right)^{\frac{\alpha}{2}} \phi}{\Gamma\left(\frac{\alpha+2}{2}, -\pi d_{\max}^2 \lambda_b\right) - \Gamma\left(\frac{\alpha+2}{2}, -\pi d_{\min}^2 \lambda_b\right)} \exp\left[-\frac{1}{2}\left(\frac{\ln 10}{10}\sigma_{\text{sh}}\right)^2\right], \tag{9}$$

where $d_{\min}, d_{\max}$ is the minimum and maximum distance between the user and the BS that it accesses respectively.

Because the uplink throughput is not affected by the BS transmission power, we only consider the downlink throughput in this paper. The lower bound of the downlink ergodic throughput received by kth user from BS_i is

$$\begin{aligned} R_{i,k}(t) &\geqslant \underline{R}_{i,k}(t) = B\log_2\left(1 + \boldsymbol{E}[\theta_{i,k}]\right) \\ &\approx B\log_2\left(1 + \frac{\boldsymbol{E}\left[\beta_{(i,k)}\right] P_{\text{t}(i,k)}(t)(M - K_i(t))}{\sigma^2 K_i(t)}\right), \end{aligned} \tag{10}$$

where B is the bandwidth, σ^2 is the Gaussian additive white noise, $P_{\text{t}(i,k)}$ is the transmission power of BS_i for kth user. The downlink total throughput of BS_i at the time slot t can be represented as $R_{(i)-\text{sum}}(t)$, $R_{(i)-\text{sum}}(t) = \sum_{k=1}^{K_i(t)} R_{i,k}(t)$. The total downlink ergodic throughput of the solar-powered cellular network $R_{\text{sum}}(t)$ is the sum of the ergodic throughput of all BSs collected in the micro-grid, which can be formulated as

$$\begin{aligned} R_{\text{sum}}(t) &= \sum_{i=1}^{N}\sum_{k=1}^{K_i(t)} B\log_2\left(1 + \frac{\boldsymbol{E}\left[\beta_{(i,k)}\right] P_{\text{t}(i,k)}(t)(M - K_i(t))}{\sigma^2 K_i(t)}\right) \\ &= \sum_{i=1}^{N}\sum_{k=1}^{K_i(t)} \underline{R}_{i,k}(t). \end{aligned} \tag{11}$$

The total transmission power $P_{\text{T}(i)-\text{sum}}(t)$ of BS_i at the time slot t is the sum of the transmission power of the BS to all accessed users at the time slot t, i.e., $P_{\text{T}(i)-\text{sum}}(t) = \sum_{k=1}^{K_i(t)} P_{\text{t}(i,k)}(t)$.

The downlink power consumption of the BS is generally divided into two types: the power consumption of the power amplifier and the static power consumption P_{static} [34]. The former is related to the transmission power of the BS and is affected by the load, while the latter is related to the power consumption of the circuit P_{circuit}. So the power consumption model of the BS is

$$P_i(t) = N_{\text{Trx}}\left(P_{\text{static}} + \Delta_P P_{\text{T}(i)-\text{sum}}(t)\right), \tag{12}$$

where Δ_P is the efficiency of power amplifier, N_{Trx} is the number of multiple transceivers.

2.4 Energy sharing model

Since the BSs are connected by power lines, the energy generated by solar power can be shared through power lines in the DC micro-grid. Moreover, batteries of BSs can be charged/discharged. The average available renewable power of BS_i at the time slot t is calculated as

$$P_{\text{available}(i)}(t) = P_{\text{RE}(i)}(t) + \gamma\sum_{j\neq i}^{N} P_{ji}(t) - \sum_{j\neq 1}^{N} P_{ij}(t) - C_i(t) + \mu D_i(t), \tag{13a}$$

$$\text{s.t. } P_{ij}(t) \geqslant 0,\ C_i(t) \geqslant 0,\ D_i(t) \geqslant 0,\ \forall i \in N, \tag{13b}$$

$$P_{ij}(t) \times P_{ji}(t) = 0,\ \forall i, j \in N, \tag{13c}$$

where $P_{ji}(t) \in \boldsymbol{P}_{\text{ex}}(t)$, $1 \leqslant i \leqslant N$, $1 \leqslant j \leqslant N$ is the shared power from BS_j to BS_i at the time slot t. $\boldsymbol{P}_{\text{ex}}(t) \in \mathbb{R}^{N\times N}$ is the average shared power matrix of the cellular network at the time slot t. $\mathbb{R}$ represents the set of real numbers. $\mathbb{R}^{N\times N}$ represents the $N \times N$ dimensional matrix in the real number domain. γ is the efficiency of power lines.

3 Modeling and optimization of CE of cellular network

Energy efficiency only shows the relationship between the consumption of energy by a network and its performance, rather than the relationship between its carbon emissions and performance. To better evaluate the trade-off between network carbon emissions and performance, this section introduces the concept of CE. CE of cellular networks can be defined as the ratio between the performance of a network and the carbon emissions it generates. Therefore, we define the CE as the ratio of the total downlink throughput of cellular networks to the carbon emissions generated by cellular networks whose units are in bps/kg. We use the carbon emission factor specified by the intergovernmental panel on climate change (IPCC) [35] to calculate the carbon emission. Therefore, the carbon emission per unit time of cellular networks in the use phase is calculated as

$$\begin{aligned}\mathrm{CF}(t) =&\kappa_{\mathrm{grid}} E_{\mathrm{grid}}\ (t) + \kappa_{\mathrm{re}} E_{\mathrm{con\_re}}(t)\\ =&\kappa_{\mathrm{grid}} \Delta t P_{\mathrm{grid}}(t) + \kappa_{\mathrm{re}} \Delta t P_{\mathrm{con\_re}}(t)\\ =&\kappa_{\mathrm{grid}} P_{\mathrm{grid}}(t) + \kappa_{\mathrm{re}} P_{\mathrm{con\_re}}(t),\end{aligned} \tag{14}$$

where the Δt is the unit time which can be ignored.

We define the energy of the city grid as traditional energy. E_{grid} is the traditional energy consumption of the cellular network at time slot t, $\kappa_{\mathrm{grid}}, \kappa_{\mathrm{re}}$ is the carbon emission factor of the traditional grid and the renewable source. P_{grid} is the average traditional power consumption of the cellular network at the time slot t, calculated as the sum of the average traditional power consumption of all BSs in cellular networks, $P_{\mathrm{grid}}(t) = \sum_{i=1}^{N} P_{\mathrm{grid}(i)}(t)$, $P_{\mathrm{grid}(i)}(t)$ is the average traditional power consumption of the BS_i at the time slot t. $P_{\mathrm{con\_re}}(t) = \sum_{i=1}^{N} P_{\mathrm{con\_re}(i)}(t)$ is the average renewable power consumption of the BS_i at the time slot t.

The average traditional power consumed by the BS_i at time slot t is

$$P_{\mathrm{grid}(i)}(t) = \max\left(P_i(t) - P_{\mathrm{available}(i)}(t), 0\right), \tag{15}$$

where $P_{\mathrm{available}(i)}(t)$ is the available renewable power of the BS_i at time slot t. Eq. (15) means that when the the available renewable power is greater than the power consumption of BS_i, the traditional power is not be consumed by BS_i. Otherwise, the traditional power is used to make up the part of available renewable power that is less than the power consumption of BS_i.

The renewable power consumed by BS_i at time slot t is

$$P_{\mathrm{con\_re}(i)}(t) = \min\left(P_i(t), P_{\mathrm{available}(i)}(t)\right). \tag{16}$$

Eq. (16) indicates that when the available renewable power of BS_i is less than the power consumption of BS_i, BS_i consumes all the available renewable power. Otherwise, the renewable power consumed by BS_i is equal to the power consumption of BS_i, that is, the available renewable energy power consumed by BS_i cannot exceed its power consumption.

Then the CE of cellular networks is

$$\eta_{\mathrm{CE}}(t) = \frac{R_{\mathrm{sum}}(t)}{\mathrm{CF}(t)}. \tag{17}$$

Combined with the content of Section 2, the CE optimization model is established as

$$\max_{\boldsymbol{P}_{\mathrm{t}}, \boldsymbol{P}_{\mathrm{ex}}, \boldsymbol{C}, \boldsymbol{D}} \quad \eta_{\mathrm{CE}}(t) = \frac{R_{\mathrm{sum}}(t)}{\mathrm{CF}(t)}, \tag{18a}$$

$$\text{s.t.} \quad P_{ij}(t) \geqslant 0,$$

$$C_i(t) \geqslant 0,\ D_i(t) \geqslant 0,\ \forall i, j \in N, \tag{18b}$$

$$P_{ij}(t) \times P_{ji}(t) = 0,$$

$$C_i(t) \times D_i(t) = 0,\ \forall i, j \in N, \tag{18c}$$

$$E_{\mathrm{Bmin}} \leqslant B_i(t) \leqslant E_{\mathrm{Bmax}},\ \forall i \in N, \tag{18d}$$

$$R_{i,k}(t) \geqslant R_{\mathrm{req}(k)},\ \forall i \in N,\ \forall k \in K_i(t), \tag{18e}$$

$$P_{T(i)-\mathrm{sum}}(t) \leqslant P_{\mathrm{tmax}},\ \forall i \in N, \tag{18f}$$

Algorithm 1 CE optimization algorithm for cellular networks

Require: Generation power of renewable source at the time slot t $P_{\mathrm{RE}}(t)$; BS static power P_{S}; the power consumption of AC loads P_{AC}.
Ensure: Energy sharing matrix $\boldsymbol{P}_{\mathrm{ex}}$; charge and discharge matrix $\boldsymbol{C}$, $\boldsymbol{D}$; transmission power allocation matrix $\boldsymbol{P}_{\mathrm{t}}$.
Initialize: $\boldsymbol{P}_{\mathrm{ex}} = 0$; number of iterations $I = 1000$;
  Repeat :
    Calculate the transmission power allocation matrix $\boldsymbol{P}_{\mathrm{t}}$ to maximize CE η_{CE};
    Calculate the energy sharing matrix $\boldsymbol{P}_{\mathrm{ex}}$ and the charge and discharge matrix $\boldsymbol{C}$, $\boldsymbol{D}$, transmission power allocation matrix $\boldsymbol{P}_{\mathrm{t}}$ to maximize carbon efficiency η_{CE};
    Calculate the CE $\eta_{\mathrm{CE}}(j) = \frac{R_{\mathrm{sum}}}{\mathrm{CF}}$;
    if $j < I$
      $j = j + 1$;
    else
      Break;
    end if
  Until $\eta_{\mathrm{CE}}(j) - \eta_{\mathrm{CE}}(j-1) < \epsilon$;
$\eta_{\mathrm{CE}}(j)$ is the optimal CE.

where the constraint (18b) represents that in the process of energy sharing among BSs and charging/discharging of batteries, the shared power and the charged/discharged power should be non-negative. Constraint (18c) means that in the process of energy sharing, due to the limitation of power lines, there can only be one energy flow in the power line between BS_i and BS_j at the same time, and the batteries in the same BS cannot be charged and discharged at the same time. Constraints (18d) means the energy of batteries is limited by the upper charge threshold and the lower discharge threshold. $R_{\mathrm{req}(k)}$ stands for the kth user's quality of service (QoS) requirement. In this paper, $R_{\mathrm{req}(k)}$ is defined as the throughput requirement. Eq. (18e) means that the ergodic downlink throughput of the cellular network must ensure the user's QoS requirements. P_{tmax} is the maximum transmission power of BSs. Constraint (18f) means that the transmission power of BSs cannot exceed the maximum transmission power.

To facilitate the solution, the method in [8] proves that the constraint (18c) can be ignored. Then the optimization problem (18) is equivalent to the optimization problem Eq. (19)

$$\max_{\boldsymbol{P}_{\mathrm{t}},\boldsymbol{P}_{\mathrm{ex}},\boldsymbol{C},\boldsymbol{D}} \quad \eta_{\mathrm{CE}}(t) = \frac{R_{\mathrm{sum}}(t)}{\mathrm{CF}(t)}, \tag{19a}$$

$$\text{s.t.} \quad P_{ij}(t) \geqslant 0,$$

$$C_i(t) \geqslant 0, D_i(t) \geqslant 0,\ \forall i, j \in N, \tag{19b}$$

$$E_{\mathrm{Bmin}} \leqslant B_i(t) \leqslant E_{\mathrm{Bmax}},\ \forall i \in N, \tag{19c}$$

$$R_{i,k}(t) \geqslant R_{\mathrm{req}}\ ,\ \forall i \in N,\ \forall k \in K_i(t), \tag{19d}$$

$$P_{\mathrm{T}(i)-\mathrm{sum}}(t) \leqslant P_{\mathrm{tmax}},\ \forall i \in N. \tag{19e}$$

The solution of the optimization problem (19) is shown as Algorithm 1.

Because of the coupling of energy sharing and charge/discharge algorithm with transmission power allocation algorithm, it is difficult to directly solve optimization problem (19). Therefore, we introduce an alternate optimization solution and divide the optimization problem (19) into two parts: the CE optimization problem based on transmission power allocation algorithm in (20) and the CE optimization problem based on energy sharing and charge/discharge algorithm in (21). The two models are solved alternately until the CE of cellular networks converges. The optimization problem (20) and the optimization problem (21) are shown as follows:

$$\max_{\boldsymbol{P}_{\mathrm{t}}} \quad \eta_{\mathrm{CE}}(t) = \frac{R_{\mathrm{sum}}(t)}{\mathrm{CF}(t)}, \tag{20a}$$

$$\text{s.t.} \quad R_{i,k}(t) \geqslant R_{\mathrm{req}}\ ,\ \forall i \in N,\ \forall k \in K_i(t), \tag{20b}$$

$$P_{\mathrm{T}(i)-\mathrm{sum}}(t) \leqslant P_{\mathrm{tmax}},\ \forall i \in N. \tag{20c}$$

In the optimization problem (20), it is supposed that the optimal energy sharing and charge/discharge strategy is known, and the transmission power allocation algorithm to maximize the CE needs to be found.

$$\max_{\boldsymbol{P}_{\mathrm{ex}},\boldsymbol{C},\boldsymbol{D}} \quad \eta_{\mathrm{CE}}(t) = \frac{R_{\mathrm{sum}}(t)}{\mathrm{CF}(t)}, \tag{21a}$$

$$\text{s.t.} \quad P_{ij}(t) \geqslant 0,\ C_i(t) \geqslant 0,\ D_i(t) \geqslant 0,\ \forall i,j \in N, \tag{21b}$$

$$E_{\text{Bmin}} \leqslant B_i(t) \leqslant E_{\text{Bmax}},\ \forall i \in N. \tag{21c}$$

In the optimization problem (21), it is assumed that the BS transmission power allocation matrix is known, and an energy sharing and charge/discharge algorithm to maximize the CE of cellular networks needs to be found.

Based on the Dinkelbach algorithm [36], we can simplify the optimization problem P3 and obtain Theorem 1 as follows.

Theorem 1. Optimization problem (20) has an optimal CE value $\eta_{\text{CE}}^*(t)$ if and only if the equation (22) is established

$$\begin{aligned} \max_{\boldsymbol{P}_\text{t}} \quad & R_{\text{sum}}\left(\boldsymbol{P}_\text{t}\right) - \text{CF}\left(\boldsymbol{P}_\text{t}\right)\eta_{\text{CE}}^* \\ & = R_{\text{sum}}\left(\boldsymbol{P}_\text{t}^*\right) - \text{CF}\left(\boldsymbol{P}_\text{t}^*\right)\eta_{\text{CE}}^* \\ & = 0, \end{aligned} \tag{22}$$

where $\boldsymbol{P}_\text{t}^*$ is the optimal power allocation policy.

Proof. See Appendix A for proof.

According to Theorem 1, the transmission power allocation problem can be transformed into an optimization problem (23) as follows:

$$\max_{\boldsymbol{P}_\text{t}} \quad R_{\text{sum}}\left(\boldsymbol{P}_\text{t}\right) - \text{CF}\left(\boldsymbol{P}_\text{t}\right)\eta_{\text{CE}} \tag{23a}$$

$$\text{s.t.} \quad R_{i,k}(t) \geqslant R_{\text{req}(k)},\ \forall i \in N,\ \forall k \in K_i(t), \tag{23b}$$

$$P_{\text{T}(i)\_\text{sum}}(t) \leqslant P_{\text{tmax}},\ \forall i \in N. \tag{23c}$$

The Lagrangian duality problem of the optimization problem (23) can be established as

$$\begin{aligned} \min_{\gamma,\gamma} L_2\left(\boldsymbol{P}_t, \eta_{\text{CE}},\ \chi, \gamma\right) = & \min_{\chi,\gamma}\max_{P_i} C_{\text{sum}}\left(\boldsymbol{P}_\text{t}\right) - \eta_{\text{CE}}\text{CF}\left(\boldsymbol{P}_\text{t}\right) \\ & + \chi\left(P_{\text{t max}} - P_{\text{t}(i,k)}(t)\right) + \gamma\left(C\left(\boldsymbol{P}_\text{t}\right) - R_{\text{req}(k)}\right) \\ = & \min_{\gamma,\gamma}\max_{P_i} \sum_{i=1}^{N}\sum_{k=1}^{K_i} \boldsymbol{E}\left[B\log_2\left(1 + \frac{\beta_{(i,k)}P_{\text{t}(i,k)}(t)}{\sigma^2}\right)\right] \\ & - \eta_{\text{CE}}\left(\kappa_{\text{grid}}P_{i,\text{grid}}(t) + \kappa_{\text{re}}\ P_{i,\text{con\_re}}(t)\right) \\ & + \sum_{i=1}^{N}\chi_i\left(P_{\text{t max}} - \sum_{k=1}^{K_i}P_{\text{t}(i,k)}(t)\right) \\ & + \sum_{i=1}^{N}\sum_{k=1}^{K_i}\gamma_k\left(\boldsymbol{E}\left[B\log_2\left(1 + \frac{\beta_{(i,k)}P_{\text{t}(i,k)}(t)}{\sigma^2}\right)\right] - R_{\text{req}(k)}\right) \end{aligned} \tag{24a}$$

$$\text{s.t.} \quad \chi_i \geqslant 0, \tag{24b}$$

$$\gamma_k \geqslant 0. \tag{24c}$$

Since there is no fixed express of $P_{\text{grid}(i)}(t)$ and $P_{\text{con\_re}(i)}(t)$, there are two cases to solve the optimization problem (24). In these two cases, the way to solve this problem is the same.

The first case is that the available renewable power of BS_i is less than the power consumption of BS_i, that is $P_{\text{available}(i)}(t) \leqslant P_i(t)$. In this case, the model of $P_{\text{grid}(i)}(t)$ and $P_{\text{con\_re}(i)}(t)$ is shown in Eq. (25).

$$P_{\text{grid}(i)}(t) = P_i(t) - P_{\text{available}(i)}(t), \tag{25a}$$

$$P_{\text{con\_re}(i)}(t) = P_{\text{available}(i)}(t). \tag{25b}$$

In this case, we solve the problem according to KKT (Karush-Kuhn-Tucker) conditions [37], and finally get the power allocation strategy as follows:

$$P_{\text{t}(i,k)}^* = \left[\frac{B\left(1+\gamma_k\right)}{\ln 2\left(\Delta_p\kappa_{\text{grid}}\eta_{\text{CE}} - \chi\right)} - \frac{\sigma^2}{\beta_{(i,k)}}\right]^+. \tag{26}$$

Algorithm 2 Transmission power allocation algorithm to maximize CE

Require: BS available power at the time slot t $P_{\text{available}}(t)$; BS static power P_{S}; the power consumption of AC loads P_{AC}.
Ensure: The transmission power allocation matrix at the time slot t $\boldsymbol{P}_{\text{t}}$.
Initialize: Maximum tolerance error ϵ; number of iterations $I = 1000$; $\eta_{\text{CE}}(0) = 0$;
  Repeat:
    Calculate the transmission power allocation matrix $\boldsymbol{P}_{\text{t}}$ to maximize $R_{\text{sum}}(\boldsymbol{P}_{\text{t}}) - \text{CF}(\boldsymbol{P}_{\text{t}})\eta_{\text{CE}}(i)$;
    if $R_{\text{sum}}(\boldsymbol{P}_{\text{t}}) - \text{CF}(\boldsymbol{P}_{\text{t}})\eta_{\text{CE}}(i) > \epsilon$ and $i < I$;
      $\eta_{\text{CE}}(i+1) = \frac{R_{\text{sum}}}{\text{CF}}$;
      $i = i + 1$;
    else
      Break;
    end if
  Until $R_{\text{sum}}(\boldsymbol{P}_{\text{t}}) - \text{CF}(\boldsymbol{P}_{\text{t}})\eta_{\text{CE}}(i) \leqslant \epsilon$;
$\boldsymbol{P}_{\text{t}}^{*} = \boldsymbol{P}_{\text{t}}$.

The second case is that the available renewable power of BS_i is more than the power consumption of BS_i, that is $P_{\text{available}(i)}(t) > P_i(t)$. In this case, the model of $P_{\text{grid}(i)}(t)$ and $P_{\text{con\_re}(i)}(t)$ is shown in

$$P_{\text{grid}(i)}(t) = 0, \tag{27a}$$

$$P_{\text{con\_re}(i)}(t) = P_i(t). \tag{27b}$$

In this case, we also solve the problem according to KKT conditions, and finally get the power allocation strategy as follows:

$$P_{\text{t}(i,k)}^{*} = \left[\frac{B\left(1+\gamma_k\right)}{\ln 2\left(\Delta_p \kappa_{\text{re}} \eta_{\text{CE}} - \chi\right)} - \frac{\sigma^2}{\beta_{(i,k)}}\right]^{+}. \tag{28}$$

The gradient descent method is used to get Lagrange multipliers.

$$\chi_i^{t+1} = \left[\chi_i^t - \delta(t)\left(P_{\text{tmax}} - P_{\text{T}(i)\_\text{sum}}(t)\right)\right]^{+}, \tag{29}$$

$$\gamma_k^{t+1} = \left[\gamma_k^t - \delta(t)\left(R_{i,k}(t) - R_{\text{req}}\right)\right]^{+}. \tag{30}$$

Until the Lagrange multipliers converge, the optimal power allocation matrix is obtained.

Therefore, the transmission power allocation algorithm to maximize the CE is shown in Algorithm 2.

Since the total downlink throughput R_{sum} of cellular networks is unrelated to energy sharing and charge/discharge algorithm, it can be regarded as a constant in the optimization problem (21). Therefore, the optimization objective of the optimization problem (21) can be simplified as follows:

$$\min_{\boldsymbol{P}_{\text{ex}},\boldsymbol{C},\boldsymbol{D}} \text{CF}(t) \quad = \kappa_{\text{grid}} \Delta t P_{\text{grid}}(t) + \kappa_{\text{re}} \Delta t P_{\text{con\_re}}(t). \tag{31}$$

Therefore, the problem of energy sharing and charge/discharge algorithm can finally be formulated as

$$\min_{\boldsymbol{P}_{\text{ex}},\boldsymbol{C},\boldsymbol{D}} \text{CF}(t) \quad = \kappa_{\text{grid}} \Delta t P_{\text{grid}}(t) + \kappa_{\text{re}} \Delta t P_{\text{con\_re}}(t), \tag{32a}$$

$$\text{s.t.} \quad P_{ij}(t) \geqslant 0,\ C_i(t) \geqslant 0,\ D_i(t) \geqslant 0,\ \forall i, j \in N, \tag{32b}$$

$$E_{\text{Bmin}} \leqslant B_i(t) \leqslant E_{\text{Bmax}},\ \forall i \in N. \tag{32c}$$

The optimization problem (32) can be considered a constrained linear programming optimization problem, which can be solved directly by the interior point method [37]. Based on it, an energy sharing and charge/discharge algorithm is designed shown in Algorithm 3.

There are two algorithms involved in this section, the transmission power allocation algorithm and the energy sharing and charge/discharge algorithm. The transmission power allocation algorithm mainly uses the Lagrangian dual equation to solve, and its complexity is $O\left(\sum_N K_i\right)$. The energy sharing and charge/discharge algorithm is mainly solved by the linear programming scheme in convex optimization, and its complexity is $O(N^3)$.

4 Simulation analysis

The simulation parameters are shown in Table 2 [34, 38, 39]. The carbon emission factor of the grid in central China specified by IPCC is selected.

Algorithm 3 Energy sharing and charge/discharge algorithm to maximize CE

Require: Generation power of renewable source at the time slot t $P_{\mathrm{RE}}(t)$; BS static power P_{S}; the power consumption of AC loads P_{AC}; the transmission power allocation matrix at the time slot t $\boldsymbol{P}_{\mathrm{t}}(t)$.

Ensure: BS available power at the time slot t $P_{\mathrm{available}}(t)$; energy sharing matrix $\boldsymbol{P}_{\mathrm{ex}}$; charge and discharge matrix C, D.

1: **Initialize:** Number of iterations $I = 1000$; iteration step size δ; initialize the penalty factor r^0; select initial $\boldsymbol{P}_{\mathrm{ex}}^0$, C^0, D^0 in the feasible domain; approximate parameter m, $i = 0$;

2: Constructing a penalty function $\Omega(u) = -\left(\frac{1}{m}\right)\log(-u)$;

3: The constrained optimization problem is transformed into an unconstrained optimization problem

$$\min f(\boldsymbol{P}_{\mathrm{ex}}^i, \boldsymbol{C}^i, \boldsymbol{D}^i, r^i) = \Delta t \sum_{n=1}^{N} |P_C + \Delta_P P_{T(i)\mathrm{sum}}(t) - P_{\mathrm{available}(i)}(t)| + r^i(\Omega(\boldsymbol{P}_{\mathrm{ex}}^i) + \Omega(\boldsymbol{C}^i) + \Omega(\boldsymbol{D}^i) + \Omega(\boldsymbol{C}^i, \boldsymbol{D}^i));$$

4: **Repeat:**

5: Solve the unconstrained optimization problem $\min f\left(\boldsymbol{P}_{\mathrm{ex}}^i, \boldsymbol{C}^i, \boldsymbol{D}^i, r^i\right)$;

6: $r^{i+1} = \delta r^i$;

7: **Untill** $r^i\Omega(\boldsymbol{P}_{\mathrm{ex}}^i, \boldsymbol{C}^i, \boldsymbol{D}^i) < \epsilon$.

Table 2 Simulation parameters

Parameter	Value
BS Static power consumption P_{static}	130 Watt [34]
BS transmission power slope Δ_P	4.7 [34]
The number of multiple transceivers N_{Trx}	6 [34]
Upper charge threshold E_{Bmax}	2000 Wh
Lower discharge threshold E_{Bmin}	250 Wh
Total area of solar photovoltaic panels A	2.256 m × 1.133 m
Photovoltaic panel efficiency λ	21.12%
Path loss coefficient α	2 [38]
White Gaussian noise σ^2	−174 dBm [39]
BS maximum transmission power P_{tmax}	47 dBm [34]
Maximum tolerance error ϵ	0.01
Number of iterations I	1000
Number of BS antennas M	128
Charge/discharge efficiency μ	95%
Transmission efficiency of power lines β	95%
Carbon emission factor of renewable energy κ_{re}	0.05 g/Wh
Carbon emission factor of traditional energy κ_{grid}	0.5703 g/Wh
User downlink bandwidth B	5 Mhz
The density of BS λ_b	$0.00001/\mathrm{m}^2$
The nearest distance between BS and user d_{min}	1 m
The farthest distance between BS and user d_{min}	500 m
The area of the cellular network	500 m × 500 m
The constant related to the carrier frequency and the antenna gain ϕ	1
The Variance of log-normal shadow fading σ_{sh}^2	10 dB

In this scenario, it is assumed that users always connect to the nearest BS [38]. The initial battery energy is denoted as B_{initial}, which represents the battery energy level at the start of the simulation.

The generation model of solar energy established in Section 2 is used to simulate the variation of power generated by generation systems integrated by BSs. Given the geographic proximity of the BSs, the power variation generated by their respective solar energy systems exhibits a comparable pattern. However, due to the presence of cloud cover, the power generated by these systems becomes uncertain and subject to fluctuation. It can be seen that the power generated by the generation system of each BS is uneven in spatial and temporal. Considering that the overall pattern of solar radiation for the four seasons, as demonstrated in Section 2, is similar, we select the solar radiation data from summer as a representative reference for display. Figure 3 shows the power generated by the solar energy generation system of some BSs in the cellular network calculated using (2).

In the subsequent simulation results, we make a comparison between the cellular network implementing the proposed carbon efficiency optimization algorithm (CEOA) and the cellular network employing the energy efficiency optimization algorithm (EEOA) proposed in [40] alongside a heuristic energy sharing

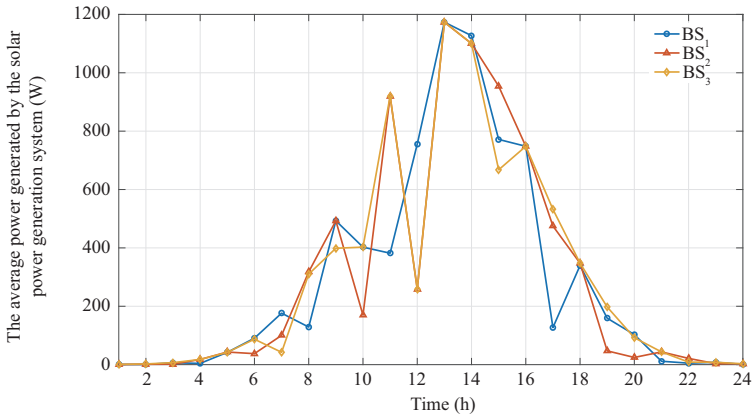

Figure 3 (Color online) Power generated by solar energy generation system.

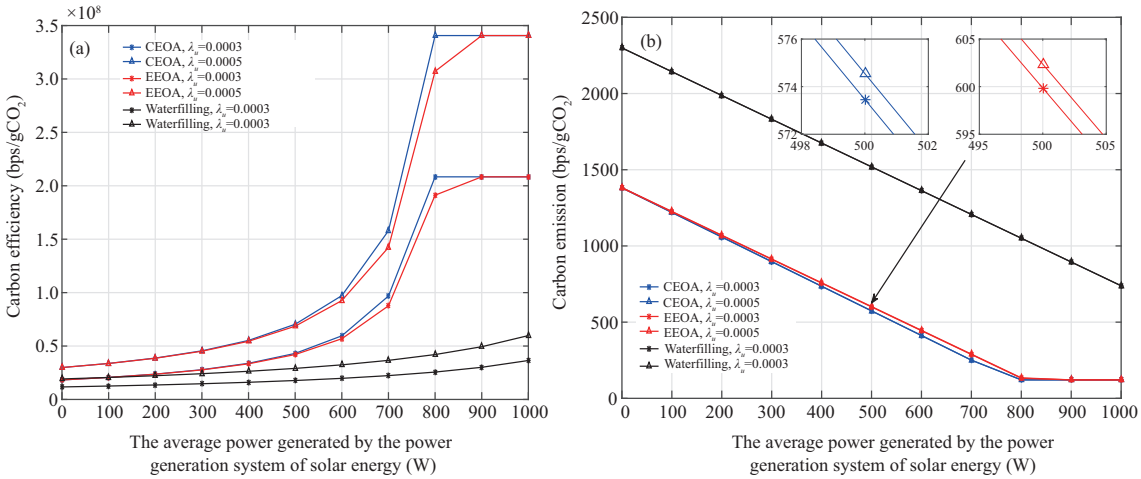

Figure 4 (Color online) (a) CE of the cellular network and (b) carbon emissions of the cellular network using CEOA, EEOA, and water filling with different density of users and different power generated by solar energy generation system. The initial battery energy $B_{\text{initial}} = 250$ Wh.

and charge/discharge algorithm proposed in [19]. Additionally, we consider the cellular network utilizing the water filling power allocation scheme in conjunction with the heuristic energy sharing and charge/discharge algorithm. To simplify the representation, we use "EEOA" to refer to the combination of EEOA and the heuristic energy sharing and charge/discharge algorithm, and we use "water filling" to encompass the water filling power allocation scheme as well as the heuristic energy sharing and charge/discharge algorithm.

Figure 4(a) presents the variation of CE for the entire network as the power generated by the solar energy generation system of each BS in the cellular network changes, considering different user densities. It can be seen from Figure 4(a), it is evident that as the power generated by the solar energy generation system increases, the CE also increases. However, once the power generated by the solar energy generation system surpasses a certain threshold, the CE reaches its maximum and remains unchanged thereafter. Besides, the CE of the cellular network using CEOA is larger than the CE of the cellular network using EEOA and the CE of the cellular network using water filling. Moreover, the greater the power generated by the solar energy generation system of each BS, the more significant the improvement in CE achieved through the adoption of CEOA. According to Algorithm 1 in Section 3, when the available renewable power of BS is more than the power consumption of this BS, the optimization objective is similar to energy efficiency, resulting in identical CE for both the cellular network utilizing CEOA and the one employing EEOA.

Figure 4(b) illustrates the variation of carbon emissions for the entire network as the power generated by the solar energy generation system of each BS in the cellular network changes, considering different user densities. It can be seen from Figure 4(b), with the increase of power generated by solar energy generation

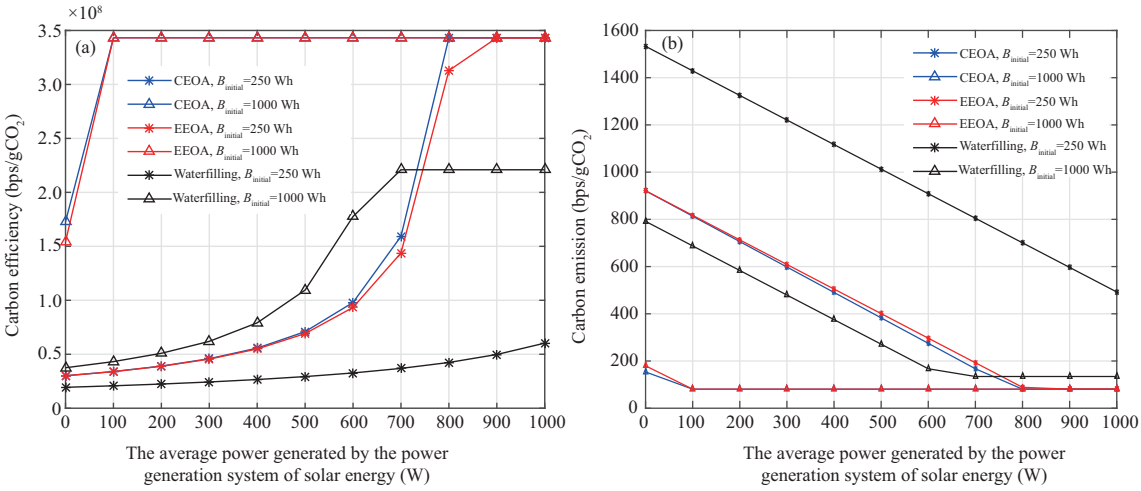

Figure 5 (Color online) (a) CE of the cellular network and (b) carbon emissions of the cellular network using CEOA, EEOA, water filling with initial battery energy and different power generated by solar energy generation system. The density of users $\lambda_u = 0.0005/\mathrm{m}^2$.

system, the carbon emissions decrease. Besides, the carbon emissions of cellular network using CEOA are less than the carbon emissions of cellular network using EEOA and the carbon emissions of cellular network using water filling in the same density of users. Additionally, the carbon emissions of the cellular network are greater with higher user density. According to the algorithm in Section 3, when the available renewable power of BS is more than the power consumption of this BS, the optimization objective is similar to energy efficiency, resulting in identical carbon emissions for both the cellular network utilizing CEOA and the one employing EEOA.

Figure 5(a) shows the CE of the entire network as it varies with the power generated by the solar energy generation system and the initial battery energy of each BS within the cellular network. It can be seen from Figure 5(a), with the increase of power generated by solar energy generation system, the CE increases. However, once the power generated by the solar energy generation system surpasses a certain threshold, the CE reaches its maximum value and remains unchanged thereafter. Additionally, the larger the initial battery energy, the smaller the value of the power generated by the solar energy generation system at which the CE reaches its maximum value.

Figure 5(b) depicts the carbon emissions of the entire network as they vary with the power generated by the solar energy generation system and the initial battery energy of each base BS within the cellular network. Once the power generated by the solar energy generation system surpasses a certain threshold, the carbon emissions reach their minimum value and remain unchanged thereafter. Furthermore, it is worth noting that the larger the initial battery energy, the smaller the value of the power generated by the solar energy generation system at which the carbon emissions reach their minimum value. Additionally, from Figure 5(b), it can be observed that cellular networks with lower initial battery energy levels tend to exhibit higher carbon emissions.

Figure 6(a) shows the hourly variation in the CE of the cellular network. As observed in Figure 6(a), the implementation of the CEOA leads to an improvement in the CE of the cellular network in the simulation scenario. By utilizing CEOA, the CE of the cellular network can be enhanced by up to 2.70×10^7 bps/g when compared to the cellular network employing the EEOA. Furthermore, the CE of the cellular network can be improved by up to 2.56×10^8 bps/g when compared to the cellular network utilizing the water filling.

Figure 6(b) shows the hourly variation in the traditional power consumption of the cellular network. From Figure 6(b), it can be seen that the traditional power consumption of the cellular network in the simulation scenario is reduced when the CEOA is used. By employing CEOA, the traditional power consumption of the cellular network can be decreased by up to 72.24 Watts when compared to the cellular network utilizing the EEOA. Additionally, the traditional power consumption of the cellular network can be reduced by up to 1681.07 Watts when compared to the cellular network employing the water filling.

Figure 6(c) presents the cumulative carbon emissions of cellular networks over the course of one day. It can be seen from Figure 6(c), the cumulative carbon emissions keep increasing with time going by. During

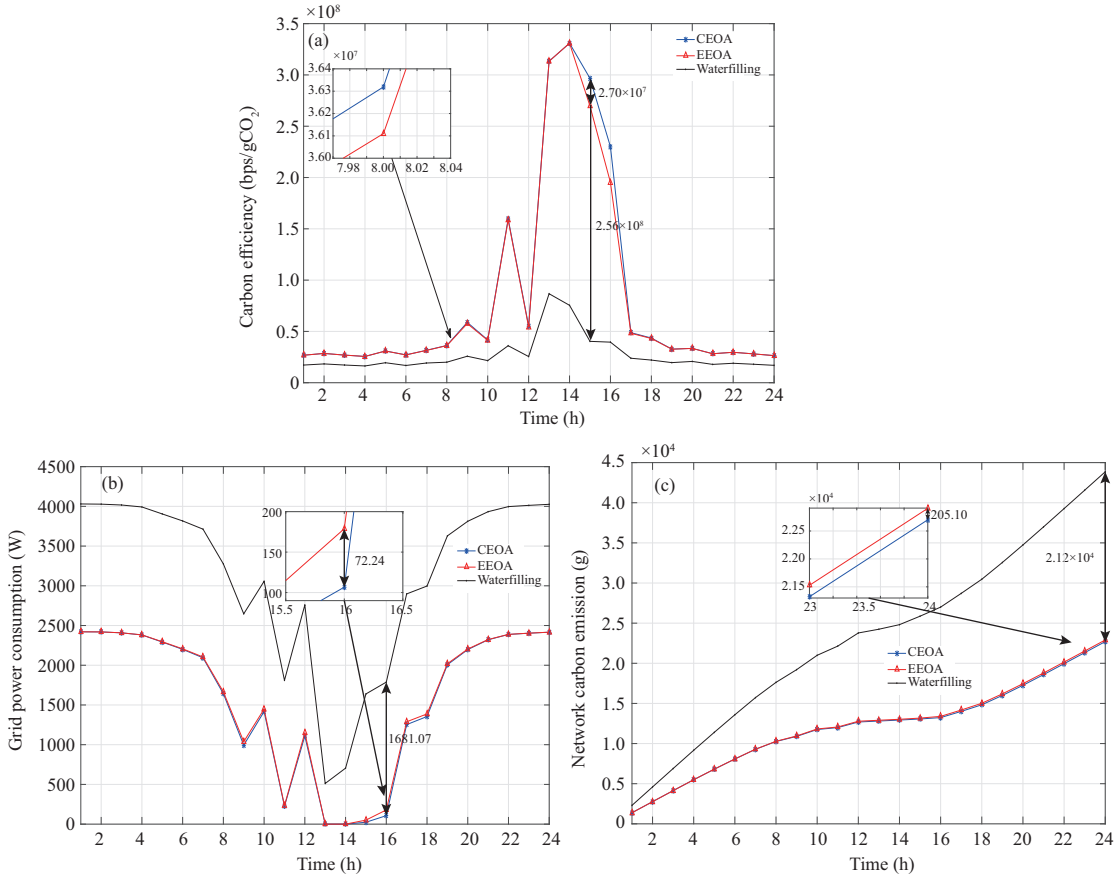

Figure 6 (Color online) (a) CE of the cellular network, (b) carbon emission of the cellular network, and (c) cumulative carbon emissions of the cellular network using CEOA, EEOA, water filling within one day. The initial battery energy $B_{\text{initial}} = 250$ Wh. The density of users $\lambda_u = 0.0005/\text{m}^2$.

noon, when the solar energy generation system produces a significant amount of power, the cumulative carbon emissions exhibit slower growth. After using the CEOA, the cumulative carbon emissions of cellular networks in a single day can be reduced by 205.10 g compared with the cellular network using EEOA. Furthermore, the cumulative carbon emissions of cellular networks in one day can be reduced by 2.12×10^4 g when compared to the cellular network employing the water filling.

In summary, the CEOA proposed in this paper effectively resolves the mismatch between the energy consumption of cellular networks and the power generation of energy networks. Through control of BS transmission power and energy sharing, CEOA can significantly lower traditional energy consumption in cellular networks, reducing carbon emissions and improving their CE. Finally, the low-carbon communication system will aid in achieving the goal of international carbon neutrality. Comparative analysis against EEOA and water filling demonstrates that CEOA yields improvements in both CE and carbon emissions. Despite the complexity of CEOA being linked to the number of users and BSs, it remains less intricate than the greedy scheme. In large-scale cellular networks, due to the complexity of CEOA, the implementation of CEOA may pose challenges, but a feasible approach involves dividing BSs into multiple sub-networks and optimizing each sub-network using CEOA. Furthermore, the comparison with the algorithm optimizing for energy efficiency reveals that the algorithm prioritizing CE as the optimization goal can achieve greater reductions in carbon emissions. This outcome underscores the efficacy of CE in better capturing the intricate relationship between carbon emissions and the performance of the cellular network compared to energy efficiency.

5 Conclusion

Because of the low-carbon requirement of cellular networks, it is a promising solution to use renewable source to supply cellular networks. However, due to the stochastic and spatial-temporal heterogeneity

inherent in renewable energy generation and cellular network energy consumption, achieving compatibility between the renewable energy network and the cellular network becomes a challenge, resulting in suboptimal utilization of renewable energy. To solve this problem, based on convex optimization and the Dinkelbach algorithm, using the idea of alternating optimization, a cellular network CE optimization algorithm is proposed. The algorithm enables each BS in the cellular network to adjust the transmission power allocation algorithm, charge/discharge algorithm of the energy storage systems occupied by BSs, and energy sharing algorithm in time according to the power generated by the solar energy and the energy in the energy storage systems and the number of users who access the cellular network. Consequently, the algorithm enhances the CE of cellular networks and reduces their carbon emissions. Simulation results demonstrate that our optimization scheme yields a maximum improvement of 2.56×10^8 bps/g in the CE of the cellular network, as compared to conventional power allocation schemes such as the traditional water filling method and heuristic energy sharing and charge/discharge algorithms.

Acknowledgements This work was supported by National Natural Science Foundation of China (Grant No. 6211001027).

References

1 L. ITU-T (01/20). Greenhouse gas emissions trajectories for the information and communication technology sector compatible with the UNFCCC paris agreement. ITU-T L.1470 (01/20), 2020. https://www.itu.int/rec/T-REC-L.1470-202001-I/en
2 Wbcsd W R I. The greenhouse gas protocol. A corporate accounting and reporting standard, 2004. https://www.wbcsd.org/Programs/Climate-and-Energy/Climate/Resources/A-corporate-reporting-and-accounting-standard-revised-edition
3 Fall M, Balboul Y, Fattah M, et al. Towards sustainable 5G networks: a proposed coordination solution for macro and pico cells to optimize energy efficiency. IEEE Access, 2023, 11: 50794–50804
4 Hassan H A H, Nuaymi L, Pelov A. Renewable energy in cellular networks: a survey. In: Proceedings of the IEEE Online Conference on Green Communications, 2013. 1–7
5 Jahid A, Hossain M S. Feasibility analysis of solar powered base stations for sustainable heterogeneous networks. In: Proceedings of the IEEE Region 10 Humanitarian Technology Conference, 2017. 686–690
6 Cai L X, Liu Y K, Luan T H, et al. Sustainability analysis and resource management for wireless mesh networks with renewable energy supplies. IEEE J Sel Areas Commun, 2014, 32: 345–355
7 Lorincz J, Garma T, Petrovic G. Measurements and modelling of base station power consumption under real traffic loads. Sensors, 2012, 12: 4281–4310
8 Chia Y K, Sun S, Zhang R. Energy cooperation in cellular networks with renewable powered base stations. IEEE Trans Wireless Commun, 2014, 13: 6996–7010
9 Jahid A, Monju M K H, Hossain M E, et al. Renewable energy assisted cost aware sustainable off-grid base stations with energy cooperation. IEEE Access, 2018, 6: 60900–60920
10 Jahid A, Hossain M S. Energy-cost aware hybrid power system for off-grid base stations under green cellular networks. In: Proceedings of the 3rd International Conference on Electrical Information and Communication Technology, 2017. 1–6
11 Farooq M J, Ghazzai H, Kadri A, et al. A hybrid energy sharing framework for green cellular networks. IEEE Trans Commun, 2016, 65: 918–934
12 Ahmed F, Naeem M, Ejaz W, et al. Renewable energy assisted traffic aware cellular base station energy cooperation. Energies, 2018, 11: 99
13 Jahid A, Islam M S, Hossain M S, et al. Toward energy efficiency aware renewable energy management in green cellular networks with joint coordination. IEEE Access, 2019, 7: 75782–75797
14 Mao Y, Zhang J, Letaief K B. Grid energy consumption and QoS tradeoff in hybrid energy supply wireless networks. IEEE Trans Wireless Commun, 2016, 15: 3573–3586
15 Lin X, Huang L, Guo C, et al. Energy-efficient resource allocation in TDMS based wireless powered communication networks. IEEE Commun Lett, 2017, 21: 861–864
16 Mao Y, Zhang J, Letaief K B. Joint base station assignment and power control in hybrid energy supply wireless networks. In: Proceedings of the IEEE Wireless Communications and Networking Conference, 2015. 1177–1182
17 Han D, Li S, Peng Y, et al. Energy sharing-based energy and user joint allocation method in heterogeneous network. IEEE Access, 2020, 8: 37077–37086
18 Piovesan N, Temesgene D A, Miozzo M, et al. Joint load control and energy sharing for autonomous operation of 5G mobile networks in micro-grids. IEEE Access, 2019, 7: 31140–31150
19 Sheng M, Zhai D, Wang X, et al. Intelligent energy and traffic coordination for green cellular networks with hybrid energy supply. IEEE Trans Veh Technol, 2016, 66: 1631–1646
20 Euttamarajah S, Ng Y H, Tan C K. Energy-efficient joint power allocation and energy cooperation for hybrid-powered comp-enabled HetNet. IEEE Access, 2020, 8: 29169–29175
21 Jahid A, Ahmad A S, Hossain M F. Energy efficient BS cooperation in DPS CoMP based cellular networks with hybrid power supply. In: Proceedings of the 19th International Conference on Computer and Information Technology, 2016. 93–98
22 Hossain M S, Jahid A, Islam K Z, et al. Towards energy efficient load balancing for sustainable green wireless networks under optimal power supply. IEEE Access, 2020, 8: 200635
23 Zhang F, Meng C, Yang Y, et al. Advantages and challenges of DC microgrid for commercial building a case study from Xiamen University DC microgrid. In: Proceedings of the 1st International Conference on DC Microgrids, 2015. 355–358
24 Diaf S, Diaf D, Belhamel M, et al. A methodology for optimal sizing of autonomous hybrid PV/wind system. Energy Policy, 2007, 35: 5708–5718
25 Fares D, Fathi M, Mekhilef S. Performance evaluation of metaheuristic techniques for optimal sizing of a stand-alone hybrid PV/wind/battery system. Appl Energy, 2022, 305: 117823
26 Molteni F, Buizza R, Palmer T N, et al. The ECMWF ensemble prediction system: methodology and validation. Quart J R Meteoro Soc, 1996, 122: 73–119
27 Alexiadis M C, Dokopoulos P S, Sahsamanoglou H S, et al. Short-term forecasting of wind speed and related electrical power. Sol Energy, 1998, 63: 61–68

28 Billinton R, Chen H. Determination of the optimum site-matching wind turbine using risk-based capacity benefit factors. IEE Proc Gener Transm Distrib, 1999, 146: 96–102
29 Li X, Chen Q. Calculation of the solar radiation inside the sunlight greenhouse using the cloud cover coefficient method. Trans CSAE, 2004, 20: 212–216
30 Ge X, Ye J, Yang Y, et al. User mobility evaluation for 5G small cell networks based on individual mobility model. IEEE J Sel Areas Commun, 2016, 34: 528–541
31 Zhong Y, Quek T Q S, Ge X. Heterogeneous cellular networks with spatio-temporal traffic: delay analysis and scheduling. IEEE J Sel Areas Commun, 2017, 35: 1373–1386
32 Ge X, Yang B, Ye J, et al. Spatial spectrum and energy efficiency of random cellular networks. IEEE Trans Commun, 2015, 63: 1019–1030
33 Jia D, Wu G, Li S, et al. Dynamic soft-frequency reuse with inter-cell coordination in OFDMA networks. In: Proceedings of the International Conference on Computer Communications & Networks, 2011. 1–6
34 Auer G, Giannini V, Desset C, et al. How much energy is needed to run a wireless network?IEEE Wireless Commun, 2011, 18: 40–49
35 Eggleston H S, Buendia L, Miwa K, et al. 2006 IPCC guidelines for national greenhouse gas inventories. 2006. https://www.ipcc-nggip.iges.or.jp/public/2006gl/
36 Dinkelbach W. On nonlinear fractional programming. Manage Sci, 1967, 13: 492–498
37 Boyd S P, Vandenberghe L. Convex Optimization. Cambridge: Cambridge University Press, 2004
38 Andrews J G, Baccelli F, Ganti R K. A tractable approach to coverage and rate in cellular networks. IEEE Trans Commun, 2011, 59: 3122–3134
39 Zhao L, Zheng K, Long H, et al. Performance analysis for downlink massive MIMO system with ZF precoding. Trans Emerging Tel Tech, 2014, 25: 1219–1230
40 Zhao L, Zhao H, Hu F, et al. Energy efficient power allocation algorithm for downlink massive MIMO with MRT Precoding. In: Proceedings of the Vehicular Technology Conference, 2013

Appendix A Proof of the Theorem 1

On the one hand, when the optimal CE value η_{CE}^{*} exists, there is an equation

$$\eta_{\mathrm{CE}}^{*}=\frac{R_{\mathrm{sum}}\left(\boldsymbol{P}_{\mathrm{t}}^{*}\right)}{\mathrm{CF}\left(\boldsymbol{P}_{\mathrm{t}}^{*}\right)}\geqslant\frac{R_{\mathrm{sum}}\left(\boldsymbol{P}_{\mathrm{t}}\right)}{\mathrm{CF}\left(\boldsymbol{P}_{\mathrm{t}}\right)}. \tag{A1}$$

Then we can get

$$\begin{cases}R_{\mathrm{sum}}\left(\boldsymbol{P}_{\mathrm{t}}\right)-\mathrm{CF}\left(\boldsymbol{P}_{\mathrm{t}}\right)\eta_{\mathrm{CE}}^{*}\leqslant 0,\\ R_{\mathrm{sum}}\left(\boldsymbol{P}_{\mathrm{t}}^{*}\right)-\mathrm{CF}\left(\boldsymbol{P}_{\mathrm{t}}^{*}\right)\eta_{\mathrm{CE}}^{*}=0.\end{cases} \tag{A2}$$

Therefore, the power allocation strategy $\boldsymbol{P}_{\mathrm{t}}^{*}$ in $R_{\mathrm{sum}}\left(\boldsymbol{P}_{\mathrm{t}}^{*}\right)-\mathrm{CF}\left(\boldsymbol{P}_{\mathrm{t}}^{*}\right)\eta_{\mathrm{CE}}^{*}=0$ is the optimal power allocation policy. On the other hand, when $\max_{\boldsymbol{P}_{\mathrm{t}}} R_{\mathrm{sum}}\left(\boldsymbol{P}_{\mathrm{t}}\right)-\mathrm{CF}\left(\boldsymbol{P}_{\mathrm{t}}\right)\eta_{\mathrm{CE}}^{*}=R_{\mathrm{sum}}\left(\boldsymbol{P}_{\mathrm{t}}^{*}\right)-\mathrm{CF}\left(\boldsymbol{P}_{\mathrm{t}}^{*}\right)\eta_{\mathrm{CE}}^{*}=0$ has an optimal power allocation strategy $\boldsymbol{P}_{\mathrm{t}}^{*}$, then have inequality:

$$R_{\mathrm{sum}}\left(\boldsymbol{P}_{\mathrm{t}}\right)-\mathrm{CF}\left(\boldsymbol{P}_{\mathrm{t}}\right)\eta_{\mathrm{CE}}^{*}\leqslant R_{\mathrm{sum}}\left(\boldsymbol{P}_{\mathrm{t}}^{*}\right)-\mathrm{CF}\left(\boldsymbol{P}_{\mathrm{t}}^{*}\right)\eta_{\mathrm{CE}}^{*}=0. \tag{A3}$$

Then we get

$$\eta_{\mathrm{CE}}^{*}=\frac{R_{\mathrm{sum}}\left(\boldsymbol{P}_{\mathrm{t}}^{*}\right)}{\mathrm{CF}\left(\boldsymbol{P}_{\mathrm{t}}^{*}\right)}\geqslant\frac{R_{\mathrm{sum}}\left(\boldsymbol{P}_{\mathrm{t}}\right)}{\mathrm{CF}\left(\boldsymbol{P}_{\mathrm{t}}\right)}. \tag{A4}$$

In this case, the optimal allocation strategy is the one that maximizes CE.